Signal Processing 140 (2017) 60–68

Contents lists available at ScienceDirect

Signal Processing

journal homepage: www.elsevier.com/locate/sigpro

Tobit Kalman filter with fading measurements☆

Hang Geng[a], Zidong Wang[b,c,*], Yan Liang[d], Yuhua Cheng[a], Fuad E. Alsaadi[e]

[a] School of Automation Engineering, University of Electronic Science and Technology of China, Chengdu 611731, China
[b] College of Electrical Engineering and Automation, Shandong University of Science and Technology, Qingdao 266590, China
[c] Department of Computer Science, Brunel University London, Uxbridge, Middlesex, UB8 3PH, United Kingdom
[d] School of Automation, Northwestern Polytechnical University, Xi'an 710129, China
[e] Faculty of Engineering, King Abdulaziz University, Jeddah 21589, Saudi Arabia

ARTICLE INFO

Article history:
Received 25 October 2016
Revised 29 March 2017
Accepted 19 April 2017
Available online 4 May 2017

Keywords:
Censored measurements
Fading channel
Kalman filter
Time delay
Tobit measurement model

ABSTRACT

This paper is concerned with the Tobit Kalman filtering problem for a class of discrete time-varying systems with both censored and fading measurements. The censored measurements are described by the Tobit measurement model and the fading measurements are characterized by the *L*th-order Rice fading channel model capable of accounting for not only the packet dropout but also the communication phenomenon. The measurement fading occurs in a random way where the fading probabilities are regulated by a set of mutually independent Gaussian random variables. By resorting to the state augmentation technique and the orthogonality projection principle, the Tobit Kalman filter (TKF) is designed in the presence of fading measurements. In the course of filter design, several state-augmentation-induced terms are introduced, all of which can be calculated recursively or off-line. A numerical example concerning the estimation of ballistic roll rates is provided to illustrate the usefulness of the proposed filter.

1. Introduction

1.1. Motivation

The past decades have witnessed the widespread applications of the filtering techniques in areas such as maneuvering target tracking, inertial navigation, global position system (GPS) positioning, and so forth [1–7]. Among a variety of filters designed under different circumstances, the Kalman filter (KF) has proven to be the most popular one. It is generally recognized that the KF is optimal in the sense of minimum mean-squared error (MMSE) under the assumption that the systems are linear and the noises are Gaussian. This assumption is, unfortunately, not always true in practice due to the fact that the nonlinearity, which serves as an important factor contributing to the complexities of the system modeling, exists in almost all the practical systems. In networked control systems, a typical kind of nonlinearities (e.g. censoring, fading, quantization and saturation) are unavoidable in the system measurements due mainly to the sudden environment changes, intermittent transmission congestions, random failures and repairs of components. In particular, censored and fading measurements are arguably two of the most frequently encountered measurement nonlinearities in engineering practice. The measurement nonlinearities, if not properly handled, could cause severe performance degradation of the traditional KF. To deal with this issue, many alternative filtering schemes have been reported, e.g., the extended Kalman filtering (EKF) [8] the unscented Kalman filtering (UKF) approaches [9,10], and the Tobit Kalman filtering method [11].

Investigating the literature concerning censored measurements, fading measurements and Kalman filtering, we can find that: (1) the TKF has gained increasing research attention due primarily to its capability of suitably processing censored measurements as well as its recursive/concise structure; (2) in networked systems, the channel fading modeled as fading/degrading measurements in both the amplitude and the phase is unavoidable because of the multipath propagation/shadowing caused by the hinder of obstacles; (3) the *L*th-order Rice fading model, as compared with the analog erasure channel model and the Rayleigh channel model, has a conciser yet simpler structure and is suitable for simultaneously representing the channel fadings, packet dropouts and communication delays. As such, a seemingly natural question is that, when the measurement transmission is subject to both censoring and fading, can we design a filter to achieve the optimal estimate of the system? Nevertheless, this appears to be a non-trivial question for the

☆ This work was supported in part by the Royal Society of the UK, the Research Fund for the Taishan Scholar Project of Shandong Province of China, National Natural Science Foundation of China under Grant 61329301, and the Alexander von Humboldt Foundation of Germany.

* Corresponding author.
E-mail addresses: ghgoahead@126.com (H. Geng), Zidong.Wang@brunel.ac.uk (Z. Wang), liangyan@nwpu.edu.cn (Y. Liang).

http://dx.doi.org/10.1016/j.sigpro.2017.04.016
0165-1684/

following two reasons: (1) it is unclear which method should be chosen to deal with the time-delays coupled in the Lth-order Rice fading model; (2) it is pretty hard to establish a modified Tobit regression model which can not only correctly handle the time-delay and fading phenomena but also help design the subsequent filter design in a recursive form. This motivates us to conduct the present research.

1.2. Contribution

In this paper, we consider the Tobit Kalman filtering problem with both censored and fading measurements. Due to the existence of time delays in the fading measurements, the system is first augmented in order to eliminate the effect of time delays. Then, the Tobit regression model in [11] is modified by taking into account the fading of the measurements. Based on the modified model and the augmented system, a modified optimal filter in the minimum mean-squared error sense (MMSE) is designed with its filter parameters explicitly characterized by the fading coefficients. Finally, the filter for the original system is obtained from the obtained modified optimal filter via some matrix manipulations.

The main contributions of this paper are highlighted as follows: *(i) to the best of the authors' knowledge, the effort made in this paper represents one of the first few attempts to deal with the filtering problem of linear discrete time-varying systems with both censored and fading measurements (which are two important types of measurement nonlinearities in networked control systems); (ii) compared with the TKF initiated in [11], several new terms arise in the filter design which are an expected reflection of the consideration of the fading measurements; and (iii) the filter presented here is of a recursive nature and is suitable for online applications.*

1.3. Related work

Censored measurements arise prevalently in a variety of applications such as biological modeling [12], economics [13–15], computer vision tracking [16] and distributed detection [17,18]. The occurrence of the censored measurements is mainly due to the fact that the measurements from sensors are often saturated as a result of dynamic changes or interferences [19]. Although receiving little attention in the filtering field, the regression of censored measurements has been extensively studied in the fields of reliability and econometrics. The Tobit model for censored measurements has been put forward by economist James Tobin in 1958 for accurately modeling household expenditure [15]. In [15], censored measurements taking the form of saturations, limits of detection and the occlusion regions are known as Tobit type 1 censoring, which can be described as a piecewise-linear transform of the output variable with a zero slope in the censored region.

The Tobit model has been intensively investigated in economics, but the corresponding Kalman filtering problem has not drawn much research attention until recently. The main difficult for designing a Kalman filter for censored measurements is that the measurement noise is non-Gaussian near the censoring region. Hence, the adoption of the standard Kalman filter will result in a biased state estimate due to the assumption that the measurement noise is zero mean Gaussian. To solve this problem, great attempts have been made in the literature, see [11,20] and the references therein. In [21], the KF was first adopted to handle censored measurements modeled by the Tobit measurement model, where the censored measurements were assumed to be independent of the true states and thus measurements in the censored region were regarded as missing. Nevertheless, it is often the case that the censored measurements described by the Tobit measurement depend heavily on the true states [11,22], and simply treating the censored measurements as missing ones may result in biased estimates. In [23], the censored and uncensored measurements were tackled separately using the iterative maximum likelihood method and all the past measurements were required in the algorithm implementation. In [11], the so-called Tobit Kalman filter (TKF) was, for the first time, developed to track the target states using censored measurements and the developed TKF was further applied to the case of two-side censoring [24]. In [19], the TKF was applied to the positioning of mobile vehicles via signals received from a number of antennas. In [22], the performance of the TKF was compared with those of EKF and UKF, and it was demonstrated that the TKF achieves more reliable and accurate state estimates for systems with censored measurements. In [20], the TKF with time-correlated multiplicative measurement noise was designed.

On another research frontier, with the rapid development of the wireless communication technology, sensors are more inclined to be connected via wireless or shared links, and the resulting networked systems has therefore attracted an ever-increasing research interest. A lot of work has been done on the networked-induced phenomena, e.g., packet dropouts, time delays, sensor saturations and quantization effects. However, the channel fading, as one of the most important networked-induced phenomena, has received relatively less attention despite its significant importance in wireless communications [25]. Generally speaking, when signals travel along the wireless links, they are susceptible to reflection, refraction and diffraction which are caused by the obstacles that hinder the propagation of the signals. In this case, signals are subject to the multiple paths phenomenon [26,27] leading to the occurrence of fading signals. Many models have been established to describe the signal variation in both the amplitude and phase in the channel fading phenomenon, for instance, the analog erasure channel model, the Rayleigh channel model and the Lth-order Rice fading channel model [28,29]. Based on these models, the problems of filter/controller design, stability analysis, simulator and emulator synthesis have been investigated in the literature.

In the past few years, a number of filter design approaches have been proposed for systems with fading measurements, see e.g. Kalman filtering [30], H_∞ filtering [31,32] and fuzzy filtering [33]. In [34], the linear-quadratic-Gaussian control problem over multiple erasure channels was studied. In [30] and [35], the finite-horizon H_∞ control for discrete time-varying nonlinear systems and the H_∞ output feedback-control for discrete-time fuzzy systems were, respectively, solved by adopting the Lth-order Rice fading model. The mean-squared stabilization problem for systems with various kinds of fading channel models was comprehensively investigated in [36] and [37]. For discrete-time multiple-input multiple-output systems, the problems of emulator design and simulator modeling over Rayleigh fading channels were tackled in [38] and [39], respectively. It should be noted that the L th-order Rice fading model gives an intuitive description of different networked-induced phenomena including the channel fading, packet dropout and communication delay.

The rest of the paper is organized as follows. In Section 2, the problem under consideration is formulated. In Section 3, the Tobit regression model is modified, based on which the optimal TKF with fading measurements is designed. In Section 4, a numerical example about estimating the ballistic roll rates is provided to show the usefulness of our filter, and some conclusions are drawn in Section 5.

Notation The notation used here is fairly standard except where otherwise stated. $\mathbb{R}^n$ denotes the n-dimensional Euclidean space. "I" and "0" respectively, represent identity matrices and zero matrices with proper dimensions. The superscripts "-1" and "T" represent inverse and transpose operations, respectively. $A^{i,j}$ and A^i represent the (i, j)th sub-block and the ith row of matrix or

variable A, respectively. $y_{1:k}$ stands for all the measurements up to time instant k. $\mathbb{E}\{x\}$ and $\mathbb{E}\{x|y\}$ will, respectively, mean expectation of x and expectation of x conditional on y. diag$\{X_m\}$ stands for a block-diagonal matrix with matrices X_m $(m = 1, 2, \ldots, M)$ on the diagonal. var$\{x\}$ denotes the variance of x.

2. Problem formulation

Consider the linear discrete time-varying system with fading measurements described by the Lth-order Rice fading model (see [30,32,33,40]) as follows:

$$x_{k+1} = A_k x_k + B_k \omega_k, \tag{1}$$

$$y_k^* = \sum_{s=0}^{\ell_k} \vartheta_k(s) C_{k-s} x_{k-s} + \upsilon_k, \tag{2}$$

where $x_k \in \mathbb{R}^{n_x}$ and $y_k^* \in \mathbb{R}^{n_y}$ are, respectively, the state vector and the uncensored measurement vector. $A_k \in \mathbb{R}^{n_x \times n_x}$, $B_k \in \mathbb{R}^{n_x \times n_\omega}$ and $C_k \in \mathbb{R}^{n_y \times n_x}$ are known time-varying matrices with appropriate dimensions. $\omega_k \in \mathbb{R}^{n_\omega}$ and $\upsilon_k \in \mathbb{R}^{n_y}$ are zero-mean and white Gaussian noises with covariances Q_k and R_k, respectively. $\ell_k = \min\{L, k\}$ where L is the order of the Lth-order Rice fading channel and k stands for the time instant. $\vartheta_k(s) \in \mathbb{R}$ $(s = 0, 1, \cdots, \ell_k)$ are the channel coefficients.

We are now in the position to introduce the Tobit measurement model (see [10,11,22]) as follows :

$$y_k = \begin{cases} y_k^*, & y_k^* > \mathcal{I}, \\ \mathcal{I}, & y_k^* \le \mathcal{I}, \end{cases} \tag{3}$$

where $y_k \in \mathbb{R}^{n_y}$ is the censored measurement vector and $\mathcal{I} = [\mathcal{I}^1 \ \mathcal{I}^2 \ \cdots \ \mathcal{I}^{n_y}]^T \in \mathbb{R}^{n_y}$ is the threshold vector, and $\mathcal{I}^m (m = 1, 2, \cdots, n_y)$ is the constant threshold of y_k^m. Depending on whether y_k is censored or not, it is assumed that (3) can be transformed into the following form:

$$y_k = \Upsilon_k y_k^* + (I - \Upsilon_k)\mathcal{I}, \tag{4}$$

where $\Upsilon_k = \text{diag}\{\gamma_k^1, \gamma_k^2, \ldots, \gamma_k^{n_y}\}$ and γ_k^m $(m = 1, 2, \ldots, n_y)$ are Bernoulli random variables which regulate the censoring phenomena of y_k^m $(m = 1, 2, \ldots, n_y)$ with the following probability distribution:

$$\text{Prob}\{\gamma_k^m = 1\} = \bar{\gamma}_k^m, \quad \text{Prob}\{\gamma_k^m = 0\} = 1 - \bar{\gamma}_k^m, \tag{5}$$

where $\bar{\gamma}_k^m$ $(m = 1, 2, \ldots, n_y)$ are known non-negative constants. It is assumed that all the random variables γ_k^m $(m = 1, 2, \ldots, n_y)$ are mutually independent, and are also uncorrelated with the fading coefficients and other noise signals.

Assumption 1. The initial state x_0 has the mean $\bar{x}_0$ and covariance P_0, and x_0, $\vartheta_k(s)$, ω_k and υ_k are mutually independent.

Assumption 2. The channel coefficients $\vartheta_k(s) = \text{diag}\{\vartheta_k^1(s), \vartheta_k^2(s), \ldots, \vartheta_k^{n_y}(s)\} (s = 0, 1, \cdots, \ell_k)$ where $\vartheta_k^m(s) (m = 1, 2, \ldots, n_y)$ are n_y uncorrelated Gaussian random variables in m and k and are also uncorrelated with other noise signals. The random variable $\vartheta_k^m(s)$, which regulates the fading phenomenon of the mth element of y_k, has the mean $\bar{\vartheta}_k^m(s)$ and variances $\tilde{\vartheta}_k^m(s)$ where $\bar{\vartheta}_k^m(s)$ and $\tilde{\vartheta}_k^m(s)$ are known.

Remark 1. As is well known, network-induced phenomena (e.g. communication delays, packet dropouts, quantization effects, sensor saturations) are ubiquitous due to the widespread applications of the networked control systems. However, the channel fading caused by the multipath propagation of the signal has not been given full consideration despite its practical significance in networked communications. To deal with the measurement fading, models such as the analog erasure channel model, the Rayleigh channel model and the Lth-order Rice fading channel model have been established [36]. It is worth mentioning that the Lth-order Rice fading model given by (2) is one of the most frequently used ones in areas of signal processing and remote control. With such a model, a few phenomenon of imperfect transmission including the channel fading and the time delay could be easily incorporated. As such, the Lth-order Rice fading model is adopted in this paper for the filter design.

Remark 2. The KF has become widely used in tracking and estimation. The KF is optimal in the sense of minimum mean-squared error when the systems are linear and the noises are Gaussian. However, in many estimation application areas, sensors are subject to a specific type of measurement nonlinearities called censoring or censored measurements because of saturated sensors, limited detection effects and image frame effects. In this case, the direct use of the KF would probably result in biased estimates because (1) the measurement noise is correlated with the state value in the censored region; and (2) the measurement noise distribution becomes censored Gaussian (instead of Gaussian), which violates the assumption of the Gaussian noise in the KF. Therefore, the KF should be modified to cater for the censored measurements. In addition, it is worth pointing out that, as two important forms of measurement nonlinearities, the censored measurements and fading measurements have not been considered simultaneously in the framework of the KF, and our main motivation is to shorten such a gap.

Remark 3. As described in (5), the random variables γ_k^m $(m = 1, 2, \ldots, n_y)$ are utilized to characterize the censoring phenomena of y_k^m $(m = 1, 2, \ldots, n_y)$. According to (4), if no censoring occurs for y_k^m, i.e., $\gamma_k^m = 1$, the measurement output is $y_k^m = (y_k^*)^m$, which implies that the output measurement is the same as the latent measurement. If the censoring phenomena occur for y_k^m, i.e., $\gamma_k^m = 0$, the measurement output is $y_k^m = \mathcal{I}^m$, which implies that the threshold is assigned to the output measurement. Here, the censoring probabilities $\bar{\gamma}_k^m$ $(m = 1, 2, \ldots, n_y)$ are assumed to be known *a priori* via some statistical experiments. Alternatively, $\bar{\gamma}_k^m$ can also approximated by (see [11]):

$$\bar{\gamma}_k^m \approx \Phi\left(\frac{\hat{\lambda}_{k|k-1}^m - \mathcal{I}^m}{\sqrt{R_k^{m,m}}}\right), \tag{6}$$

where $\hat{\lambda}_{k|k-1}^m = \sum_{s=0}^{\ell_k} \sum_{a=1}^{n_y} \sum_{b=1}^{n_x} \bar{\vartheta}_k^{m,a}(s) C_{k-s}^{a,b} \hat{x}_{k-s|k-s-1}^b$, $\bar{\vartheta}_k^{m,a}(s)$ $(m = 1, 2, \ldots, n_y, a = 1, 2, \ldots, n_y)$, $C_{k-s}^{a,b}$ $(b = 1, 2, \ldots, n_x)$ and $R_k^{m,m}$ are, respectively, the (m, a)th, (a, b)th and (m, m)th elements of $\bar{\vartheta}_k(s)$, C_{k-s} and R_k; $\hat{x}_{k-s|k-s-1}^b$ is the bth element of $\hat{x}_{k-s|k-s-1}$ which is the one-step prediction of x_{k-s}; and $\Phi(\cdot)$ is the cumulative distribution function of the random variable "$\cdot$" which obeys the standard normal distribution.

Remark 4. Nowadays, because of the advanced microprocessor technology and the fact that microprocessors can provide greater accuracy and computing power than analog computers, digital filtering methods have been more widely utilized than the classical analog filtering methods. This means that for modern filtering applications, the discrete-time filter would be more preferable. However, a thorough study of optimal filtering must include the continuous-time filter. Therefore, parallel to the discrete-time system (1)–(2) and (4), the continuous-time system is formulated as

$$\begin{aligned} \frac{dx_t}{dt} &= A_t x_t + B_t \omega_t, \\ y_t^* &= \int_0^{\ell_t} \vartheta_t(s) C_{t-s} x_{t-s} ds + \upsilon_t, \\ y_t &= \Upsilon_t y_t^* + (I - \Upsilon_t)\mathcal{I}, \end{aligned}$$

where x_t, y_t^*, y_t, ω_t, υ_t, ℓ_t, A_t, B_t, C_t, $\vartheta_t(s)$ and Υ_t are the continuous-time counterparts of x_k, y_k^*, y_k, ω_k, υ_k, ℓ_k, A_k, B_k, C_k, $\vartheta_k(s)$ and Υ_k. Based on the above continuous-time system, it would be interesting to design a continuous-time TKF to cope with censored and fading measurements, meanwhile examine the impacts from the censoring and fading phenomena on the design of the filter in the near future.

The objective of this paper is to design the optimal TKF for the discrete time-varying system (1)–(4) with censored and fading measurements.

3. Main results

In this section, we aim to establish a unified framework to solve the addressed Tobit Kalman filtering problem in the simultaneous presence of censored and fading measurements. The filter design procedure is along the similar line in [11] with two main differences: (1) a modified Tobit regression model resulting from the fading measurements; and (2) additional computations of the gain matrix and the covariance matrix, where the additional computations include the augmentation of the delayed states, calculations with respect to the augmented state and calculation of the expected values of the channel coefficients.

Rewrite system (1)–(4) in the following compact form:

$$\xi_{k+1} = \mathcal{A}_k\xi_k + \mathcal{B}_k\omega_k, \tag{7}$$

$$y_k^* = \theta_k\mathcal{C}_k\xi_k + \upsilon_k, \tag{8}$$

$$y_k = \begin{cases} \theta_k\mathcal{C}_k\xi_k + \upsilon_k, & \theta_k\mathcal{C}_k\xi_k + \upsilon_k > \mathcal{I}, \\ \mathcal{I}, & \theta_k\mathcal{C}_k\xi_k + \upsilon_k \le \mathcal{I}, \end{cases} \tag{9}$$

$$y_k = \Upsilon_k(\theta_k\mathcal{C}_k\xi_k + \upsilon_k) + (I - \Upsilon_k)\mathcal{I}, \tag{10}$$

where

$$\xi_k = \mathrm{col}\{x_k, x_{k-1}, \cdots, x_{k-\ell_k}\},$$
$$\theta_k = [\vartheta_k(0) \quad \vartheta_k(1) \quad \cdots \quad \vartheta_k(\ell_k)],$$
$$\mathcal{C}_k = \mathrm{diag}\{C_k, C_{k-1}, \cdots, C_{k-\ell_k}\},$$
$$\mathcal{A}_k = \begin{bmatrix} A_k & 0 & \cdots & 0 \\ I & 0 & \cdots & 0 \\ \vdots & \ddots & \ddots & \vdots \\ 0 & \cdots & I & 0 \end{bmatrix}, \quad \mathcal{B}_k = \begin{bmatrix} B_k \\ 0 \\ \vdots \\ 0 \end{bmatrix}.$$

Thorough the above augmentation, the system with time delays in (1) –(4) is transformed into the one in (7)–(10) without time delays.

Remark 5. In fact, many efficient approaches have been presented in the literature concerning the time delay phenomenon in the past two decades, such as the augmentation technique [41,42], the bounding technique [43], the descriptor system method [44], the slack matrix variables technique [45] and the delay-fractioning approach [46] . Generally speaking, the conservatism and complexity of the algorithm should be considered when handling the time delay phenomenon. That is to say, there should be a trade-off between the conservatism and the complexity of the proposed algorithm. Here, the conservatism means that the proposed algorithm should provide a maximal allowable delay; and the complexity means that the algorithm includes as few decision variables as possible while achieving the same maximal allowable delay. In this paper, to remove the time delay effect, the augmentation technique as shown in (7)– (10) is chosen to benefit the following filter design at the cost of some extra computational cost.

Denote y_k^m and $\mathcal{I}^m$ $(m = 1, 2, \cdots, n_y)$, respectively, as the mth elements of y_k and $\mathcal{I}$, $\theta_k^{m,\alpha}$ as the (m, α)th $(\alpha=1, 2, \cdots, n_y(\ell_k+1))$ element of θ_k, $\mathcal{C}_k^{\alpha,\beta}$ as the (α, β)th $(\beta = 1, 2, \cdots, n_x(\ell_k + 1))$ element of $\mathcal{C}_k$, and $R_k^{m,m}$ as the (m, m)th element of $R_k^{m,m}$. Let $\chi_k^m = \sum_{\alpha=1}^{n_y(\ell_k+1)}\sum_{\beta=1}^{n_x(\ell_k+1)}\theta_k^{m,\alpha}\mathcal{C}_k^{\alpha,\beta}\xi_k^\beta$. To facilitate the subsequent filter design, the Tobit regression in [11] is first modified to encompass the fading measurements as shown in the following lemma.

Lemma 1. *The mathematical expectation and variance of y_k^m $(m = 1, 2, \cdots, n_y)$ are derived as follows:*

$$\mathbb{E}\{y_k^m|x_k, R_k^{m,m}\} = \Phi\left(\frac{\chi_k^m - \mathcal{I}^m}{\sqrt{R_k^{m,m}}}\right)\left[\chi_k^m + \sqrt{R_k^{m,m}}\lambda\left(\frac{\mathcal{I}^m - \chi_k^m}{\sqrt{R_k^{m,m}}}\right)\right] + \Phi\left(\frac{\mathcal{I}^m - \chi_k^m}{\sqrt{R_k^{m,m}}}\right)\mathcal{I}^m, \tag{11}$$

$$\mathrm{Var}\{y_k^m|x_k, R_k^{m,m}\} = R_k^{m,m}\left[1 - \varphi\left(\frac{\mathcal{I}^m - \chi_k^m}{\sqrt{R_k^{m,m}}}\right)\right], \tag{12}$$

where

$$\varphi\left(\frac{\mathcal{I}^m - \chi_k^m}{\sqrt{R_k^{m,m}}}\right) = \lambda\left(\frac{\mathcal{I}^m - \chi_k^m}{\sqrt{R_k^{m,m}}}\right) \times \left[\lambda\left(\frac{\mathcal{I}^m - \chi_k^m}{\sqrt{R_k^{m,m}}}\right) - \frac{\mathcal{I}^m - \chi_k^m}{\sqrt{R_k^{m,m}}}\right], \tag{13}$$

$$\lambda\left(\frac{\mathcal{I}^m - \chi_k^m}{\sqrt{R_k^{m,m}}}\right) = \frac{\phi\left(\frac{\mathcal{I}^m - \chi_k^m}{\sqrt{R_k^{m,m}}}\right)}{1 - \Phi\left(\frac{\mathcal{I}^m - \chi_k^m}{\sqrt{R_k^{m,m}}}\right)}, \tag{14}$$

with the probability density function (pdf) and the cumulative distribution function (cdf) of the Gaussian random variable y_k^m given by the following equations:

$$\phi\left(\frac{y_k^m - \chi_k^m}{\sqrt{R_k^{m,m}}}\right) = \frac{1}{\sqrt{2\pi}}e^{-\frac{\left(y_k^m - \chi_k^m\right)^2}{2R_k^{m,m}}}, \tag{15}$$

$$\Phi\left(\frac{y_k^m - \chi_k^m}{\sqrt{R_k^{m,m}}}\right) = \int_{-\infty}^{y_k^m}\frac{1}{\sqrt{2\pi R_k^{m,m}}}e^{-\frac{\left(z_k^m - \chi_k^m\right)^2}{2R_k^{m,m}}}d_{z_k^m}. \tag{16}$$

Proof. See Appendix A. □

Remark 6. Equations (11)–(12) in Lemma 1 give the expressions of the mathematic expectation and variance of the censored and fading measurement y_k^m. Compared with the expectation and variance expressions in [11] where only the censoring phenomenon is considered, it can be observed that, due to the introduction of the fading measurements, the term $\sum_{n=1}^{n_x}C_k^{m,n}x_k^n$ (in the case that y_k is a vector instead of a scalar) in [11] is replaced by the term χ_k^m which characterizes the effect of the fading measurements. If the fading phenomenon is not taken into account, (2) becomes $y_k^* = C_kx_k + \upsilon_k$. Then, the term χ_k^m reduces to $\sum_{n=1}^{n_x}C_k^{m,n}x_k^n$, resulting in the degradation of (11) and (12) to (8) and (11) in [11], respectively.

Remark 7. Using (11)–(16), the Tobit model in [11] with only censored measurements has been extended to the one subjecting to both censored and fading measurements as shown in (4). Note that the extra fading measurements result in (1) the replacement of $\sum_{n=0}^{n_x}C_k^{m,n}x_k^n$ by χ_k^m in all the equations relative to the measurement y_k^m; and (2) several new terms that further complicate the filter design.

Let $\bar{\Upsilon}_k=\mathbb{E}\{\Upsilon_k\}=\mathrm{diag}\{\bar{\gamma}_k^1, \bar{\gamma}_k^2, \ldots, \bar{\gamma}_k^{n_y}\}$, $\bar{\theta}_k=[\bar{\vartheta}(0)\ \bar{\vartheta}(1)\ \cdots\ \bar{\vartheta}(\ell_k)]$ with its (m, α)th element being $\bar{\theta}_k^{m,\alpha}$ $(m = 1, 2, \ldots, n_y, \alpha = 1, 2, \ldots, n_y(\ell_k + 1))$ where $\bar{\vartheta}_k(s) =\mathrm{diag}\{\bar{\vartheta}_k^1(s), \bar{\vartheta}_k^2(s), \ldots, \bar{\vartheta}_k^{n_y}(s)\}$, $s = 1, \cdots, \ell_k$, and $\hat{\xi}_{k|k-1} = \mathbb{E}\{\xi_k|y_{1:k-1}\}$ with its βth $(\beta = 1, 2, \ldots,$

$n_x(\ell_k+1))$ element being $\xi^{\beta}_{k|k-1}$. Denote $\hat{x}_{k|k-1}=\mathbb{E}\{x_k|y_{1:k-1}\}$, $\hat{y}_{k|k-1}=\mathbb{E}\{y_k|y_{1:k-1}\}$, $\hat{\xi}_{k|k}=\mathbb{E}\{\xi_k|y_{1:k}\}$, $\hat{x}_{k|k}=\mathbb{E}\{x_k|y_{1:k}\}$, $\tilde{\xi}_{k|k-1}=\xi_k-\hat{\xi}_{k|k-1}$, $\tilde{x}_{k|k-1}=x_k-\hat{x}_{k|k-1}$, $\tilde{y}_{k|k-1}=y_k-\hat{y}_{k|k-1}$, $\tilde{\xi}_{k|k}=\xi_k-\hat{\xi}_{k|k}$, $\tilde{x}_{k|k}=x_k-\hat{x}_{k|k}$, $\mathcal{P}_{k|k-1}=\mathbb{E}\{\tilde{\xi}_{k|k-1}\tilde{\xi}^T_{k|k-1}\}$, $P_{k|k-1}=\mathbb{E}\{\tilde{x}_{k|k-1}\tilde{x}^T_{k|k-1}\}$, $\mathcal{P}_{k|k}=\mathbb{E}\{\tilde{\xi}_{k|k}\tilde{\xi}^T_{k|k}\}$, $P_{k|k}=\mathbb{E}\{\tilde{x}_{k|k}\tilde{x}^T_{k|k}\}$, $\Sigma_{\tilde{y}_{k|k-1}\tilde{y}_{k|k-1}}=\mathbb{E}\{\tilde{y}_{k|k-1}\tilde{y}^T_{k|k-1}\}$ and $\Sigma_{\tilde{\xi}_{k|k-1}\tilde{y}_{k|k-1}}=\mathbb{E}\{\tilde{\xi}_{k|k-1}\tilde{y}^T_{k|k-1}\}$. Let $\hat{\chi}_{k|k-1}=\bar{\theta}_k\mathcal{C}_k\hat{\xi}_{k|k-1}$ with its mth element being $\hat{\chi}^m_{k|k-1}=\sum_{\alpha=1}^{n_y(\ell_k+1)}\sum_{\beta=1}^{n_x(\ell_k+1)}\bar{\theta}^{m,\alpha}_k\mathcal{C}^{\alpha,\beta}_k\hat{\xi}^{\beta}_{k|k-1}$.

Based on Lemma 1, the optimal TKF with fading measurements can be obtained as follows.

Theorem 1. *The optimal TKF for the augmented system (7)–(10) is given by*

$$\hat{\xi}_{k|k-1}=\mathcal{A}_{k-1}\hat{\xi}_{k-1|k-1}, \tag{17}$$

$$\mathcal{P}_{k|k-1}=\mathcal{A}_{k-1}\mathcal{P}_{k-1|k-1}\mathcal{A}^T_{k-1}+\mathcal{B}_{k-1}Q_{k-1}\mathcal{B}^T_{k-1}, \tag{18}$$

$$\hat{\xi}_{k|k}=\hat{\xi}_{k|k-1}+K_k(y_k-\hat{y}_{k|k-1}), \tag{19}$$

$$\mathcal{P}_{k|k}=\mathcal{P}_{k|k-1}-\bar{\Upsilon}_k\Sigma_{\tilde{\xi}_{k|k-1}\tilde{y}_{k|k-1}}\Sigma^{-1}_{\tilde{y}_{k|k-1}\tilde{y}_{k|k-1}}\times\Sigma^T_{\tilde{\xi}_{k|k-1}\tilde{y}_{k|k-1}}, \tag{20}$$

where $\hat{\xi}_{k|k-1}$ is the one-step prediction of ξ_{k-1}, $\hat{\xi}_{k|k}$ is the estimate of ξ_k, $\mathcal{P}_{k|k-1}$ is the one-step prediction error covariance matrix, and $\mathcal{P}_{k|k}$ is the estimation error covariance matrix. The one-step measurement prediction in (19) is given by

$$\hat{y}_{k|k-1}=\bar{\Upsilon}_k\left[\hat{\chi}_{k|k-1}+\lambda\left(\frac{\mathcal{I}-\hat{\chi}_{k|k-1}}{\sqrt{R_k}}\right)\mathcal{R}_k\right]+(I-\bar{\Upsilon}_k)\mathcal{I}, \tag{21}$$

where

$$\lambda\left(\frac{\mathcal{I}-\hat{\chi}_{k|k-1}}{\sqrt{R_k}}\right)=\mathrm{diag}\left\{\lambda\left(\frac{\mathcal{I}^m-\hat{\chi}^m_{k|k-1}}{\sqrt{R^{m,m}_k}}\right)\right\}, \tag{22}$$

$\mathcal{R}_k=col\{\sqrt{R^{1,1}_k},\sqrt{R^{1,1}_k},\ldots,\sqrt{R^{n_y,n_y}_k}\}$, *and* $\sqrt{R^{m,m}_k}$ *is the* (m,m) *th element of* R_k. *The gain matrix* K_k *in (19) has the following form:*

$$K_k=\Sigma_{\tilde{\xi}_{k|k-1}\tilde{y}_{k|k-1}}\Sigma^{-1}_{\tilde{y}_{k|k-1}\tilde{y}_{k|k-1}}, \tag{23}$$

where

$$\Sigma_{\tilde{\xi}_{k|k-1}\tilde{y}_{k|k-1}}=\mathcal{P}_{k|k-1}(\bar{\Upsilon}_k\bar{\theta}_k\mathcal{C}_k)^T, \tag{24}$$

$$\Sigma_{\tilde{y}_{k|k-1}\tilde{y}_{k|k-1}}=\bar{\Upsilon}_k\bar{\theta}_k\mathcal{C}_k\mathcal{P}_{k|k-1}(\bar{\Upsilon}_k\bar{\theta}_k\mathcal{C}_k)^T+R_k\left[I-\varphi\left(\frac{\mathcal{I}-\hat{\chi}_{k|k-1}}{\sqrt{R_k}}\right)\right], \tag{25}$$

$$\varphi\left(\frac{\mathcal{I}-\hat{\chi}_{k|k-1}}{\sqrt{R_k}}\right)=\mathrm{diag}\left\{\varphi\left(\frac{\mathcal{I}^m-\hat{\chi}^m_{k|k-1}}{\sqrt{R^{m,m}_k}}\right)\right\}. \tag{26}$$

Proof. See Appendix B. □

Remark 8. Comparing the TKF in [11] with the established filter in Theorem 1, there are two main differences. The first difference is that the term $C_k\hat{x}_{k|k-1}$ in [11] (which is the product of the measurement matrix C_k and the one-step state prediction $\hat{x}_{k|k-1}$) is replaced by a new term $\hat{\chi}_{k|k-1}=\bar{\theta}_k\mathcal{C}_k\hat{\xi}_{k|k-1}$ which is now the product of the mean of the channel coefficient, the augmented measurement matrix and the predicted value of the augmented state. The second difference is the appearance of $\bar{\theta}_k$ in the calculations of $\hat{y}_{k|k-1}$ and K_k. The first difference is caused by the time-delay effect while the second difference stems from the fading channel phenomenon.

Table 1
Implementation procedure of the proposed filtering algorithm.

Input: $\bar{x}_0$ and P_0
Output: $\hat{x}_{k|k}$ and $P_{k|k}$
for $k=1,2,\ldots,$ do
  Compute the predicted parameter $\hat{\xi}_{k|k-1}$ and its error covariance matrix $\mathcal{P}_{k|k-1}$ by (17)–(18);
  Compute the predicted state estimate $\hat{x}_{k|k-1}$ and its error covariance matrix $P_{k|k-1}$ by (27)–(28);
  Compute the predicted measurement $\hat{y}_{k|k-1}$ by (21);
  Compute the parameter $\Sigma_{\tilde{\xi}_{k|k-1}\tilde{y}_{k|k-1}}$ by (24);
  Compute the parameter $\Sigma_{\tilde{y}_{k|k-1}\tilde{y}_{k|k-1}}$ by (25);
  Compute the gain matrix K_k by (23);
  Compute the updated parameter $\hat{\xi}_{k|k}$ and its error covariance $\mathcal{P}_{k|k}$ by (19)–(20);
  Compute the updated state estimate $\hat{x}_{k|k}$ and its error covariance $P_{k|k}$ by (29)–(30);
  Return $\hat{x}_{k|k}$ and $P_{k|k}$.
end

Theorem 2. *Based on the filter given in Theorem 1 for the augmented system (7)–(10), the optimal TKF for the original system (1)–(4) with both censored and fading measurements is as follows:*

$$\hat{x}_{k|k-1}=\Gamma\hat{\xi}_{k|k-1}, \tag{27}$$

$$P_{k|k-1}=\Gamma\mathcal{P}_{k|k-1}\Gamma^T, \tag{28}$$

$$\hat{x}_{k|k}=\Gamma\hat{\xi}_{k|k}, \tag{29}$$

$$P_{k|k}=\Gamma\mathcal{P}_{k|k}\Gamma^T, \tag{30}$$

where

$$\Gamma=\left[I\quad\underbrace{0\quad\cdots\quad0}_{\ell_k\text{ blocks}}\right].$$

Proof. Noticing the relationship between system (1)–(4) and system (7)–(10), we can easily obtain the result in Theorem 2 on the basis of Theorem 1. □

Combing Lemma 1 and Theorems 1–2, we have accomplished the design of the optimal TKF with both censored measurements and fading measurements. Table 1 demonstrates the implementation procedure of the proposed filtering algorithm.

Remark 9. According to Lemma 1 and Theorems 1–2, a recursive filtering scheme is established to solve the novel filtering problem for the discrete time-varying systems suffering simultaneously from censored measurements and fading measurements. System (1)–(4) under consideration is comprehensive that covers two important measurement nonlinearities, i.e., censored and fading measurements, which are often encountered in engineering applications including target tracking and networked control. The two measurement nonlinearities are dealt with in a unified yet effective framework. Compared with the work in [11], several new terms have emerged in the filter design and these terms explicitly reflect the effect of the fading channel phenomenon. To be specific, the term $\theta^{m,\alpha}_k$ in Lemma 1 and the term $\bar{\theta}_k$ in Theorem 1 characterize the effect of the channel fading. The term ξ^{β}_k in Lemma 1, the terms $\hat{\xi}_{k|k-1}$, $\hat{\xi}_{k|k}$, $\mathcal{P}_{k|k-1}$, $\mathcal{P}_{k|k}$ in Theorem 1 and the term Γ in Theorem 2 characterize the time delay effect. The term $\hat{\chi}^m_{k|k-1}$ in Theorem 1 characterize the effects of both the time-delay and the channel fading.

Remark 10. It can be seen from Lemma 1 and Theorems 1–2 that when implementing the presented Tobit Kalman filtering algorithm with fading measurements, the computation complexity mainly involves the matrix multiplication and the matrix inversion. In the

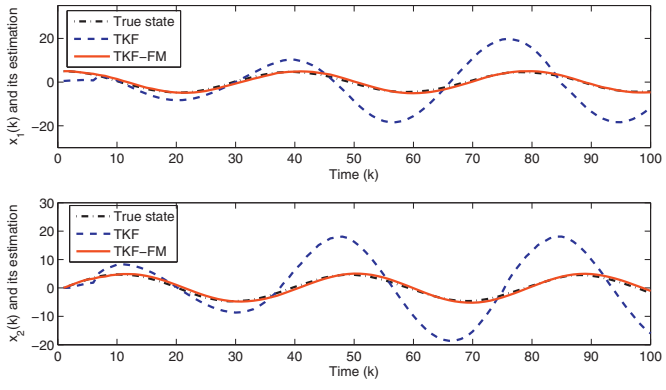

Fig. 1. True values of the first and second dimensions of the state and their estimates.

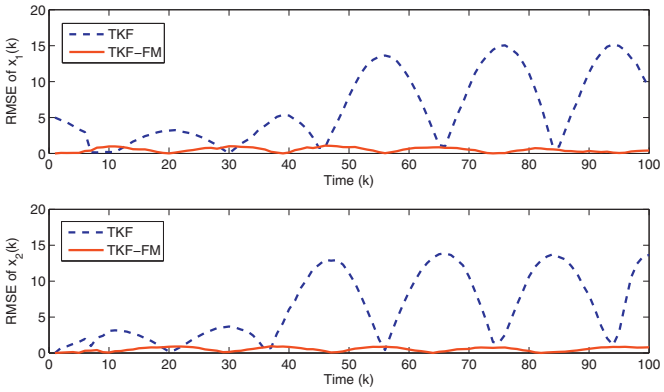

Fig. 2. Method comparison with [11] in RMSE1 and RMSE2.

matrix multiplication, the multiplication of matrices with dimensions $n_x(\ell_k+1)\times n_x(\ell_k+1)$ needs to be calculated, where n_x is the dimension of the system state; $\ell_k=\min\{L,k\}$ where L is the order of the Lth-order Rice fading channel; and k stands for the time instant. As to the matrix inversion, the inverse of matrices with dimensions $n_y\times n_y$ needs to be calculated, where n_y is the dimension of the measurement. Hence, the proposed filtering algorithm has the computational complexity of $O[(n_x(\ell_k+1))^3+(n_y)^3]$. Generally, we have $\ell_k\geq 1$ and therefore our proposed algorithm has more computation burden than the Tobit Kalman filtering algorithm in [11] which has the computational complexity of $O[(n_x)^3+(n_y)^3]$. It can be apparently seen that the extra computation burden in our algorithm is caused by the fading measurements.

4. Illustrative example

In this section, we will employ an oscillator example (modified from [11,47]) and a radar tracking example to demonstrate the effectiveness of the proposed filtering algorithm. Let RMS1 denote the root mean-squared error (RMSE) for the estimation of x_k^1, i.e., RMSE1$=\sqrt{(1/M)\sum_{j=1}^{M}(x_k^{1(j)}-\hat{x}_{k|k}^{1(j)})^2}$, where M is the number of simulation tests. Similarly, RMSE2 is the RMSE for the estimation of x_k^2, i.e., RMSE2$=\sqrt{(1/M)\sum_{j=1}^{M}(x_k^{2(j)}-\hat{x}_{k|k}^{2(j)})^2}$.

4.1. Oscillator example

Consider the following class of discrete time-varying systems given by (1)–(4) with parameters:

$$A_k=\begin{bmatrix}\cos(w) & -\sin(w)\\ \sin(w) & \cos(w)\end{bmatrix},\quad B_k=I_2,\quad w=0.052\pi,$$

$$C=\begin{bmatrix}1 & 0\end{bmatrix},\quad \bar{x}_0=\begin{bmatrix}5 & 0\end{bmatrix}^T,\quad P_0=I_2,$$

$$\bar{\vartheta}(0)=0.95,\quad \bar{\vartheta}(1)=0.75,\quad \bar{\vartheta}(2)=0.85,\quad \tilde{\vartheta}(0)=0.0081,$$

$$\tilde{\vartheta}(1)=0.0064,\quad \tilde{\vartheta}(2)=0.0049,\quad \mathcal{I}=0,$$

$$Q_k=\mathrm{diag}\{0.0025,0.0025\},\quad R_k=1,\quad L=2,$$

where $L=2$ is the order of the Rice fading channel model. The censoring probability $\bar{\Upsilon}_k=\bar{\gamma}_k^1$ can be calculated according to (6). The presented oscillator example considers the estimation of ballistic roll rates from fading and censored magnetometer data. The simulation shows a robust tracking ability with a known model and unknown disturbance that enters the system through ω_k.

Fig. 1 illustrates the true values of the states and the estimates given by the TKF in [11] and our proposed TKF with fading measurements which is named TKF-FM. Fig. 2 shows the comparison of the RMSE curves between the TKF and the TKF-FM after 1000 times of Monte Carlo simulations. From Fig. 1 we can observe that, when the measurements are subject to both censoring and fading, our proposed TKF-FM is able to track the true values of the system states while the TKF leads to significant deviations from the true state values. It can be seen from Fig. 2 that the RMSE of our TKF-FM is always smaller than that of the TKF, which is simply due to the fact that the fading measurements are properly handled in our TKF-FM while they are not addressed in the TKF.

4.2. Radar tracking example

Consider the radar tracking example with the following parameters:

$$A_k=\begin{bmatrix}1 & T & 0 & 0 & 0 & 0\\ 0 & 1 & 1 & 0 & 0 & 0\\ 0 & 0 & \varrho_1 & 0 & 0 & 0\\ 0 & 0 & 0 & 1 & T & 0\\ 0 & 0 & 0 & 0 & 1 & 1\\ 0 & 0 & 0 & 0 & 0 & \varrho_2\end{bmatrix},$$

$$C_k=\begin{bmatrix}1 & 0 & 0 & 0 & 0 & 0\\ 0 & 0 & 0 & 0 & 0 & 1\end{bmatrix},$$

$$B_k=I_6,\quad Q_k=0.25,\quad R_k=\mathrm{diag}\{100,0.001\},$$

$$x_0=\begin{bmatrix}100 & 4 & 0 & 1 & 0.001 & 0\end{bmatrix}^T,$$

$$P_0=\mathrm{diag}\{100,10,10,1,1,1\},\quad \mathcal{I}=\begin{bmatrix}100 & 1.01\end{bmatrix}^T,$$

where $x_k=[r_k\ \dot{r}_k\ u_{1,k}\ \eta_k\ \dot{\eta}_k\ u_{2,k}]$ is the target state; r_k and $\dot{r}_k$ are, respectively, the range and range rate of the target at time k; η_k and $\dot{\eta}_k$ are, respectively, the bearing and bearing rate of the target at time k; $\varrho_1=0.4$ and $\varrho_2=0.5$ are the maneuvering correlated process noises; $T=1s$ is the sampling period. The remaining parameters are the same as those in the previous example.

The performance comparison between the Tobit Kalman filter (TKF) and the proposed Tobit Kalman filter with fading measurements (TKF-FM) has been made in RMSE after 1000 times of Monte Carlo simulations. Fig. 3 illustrates the RMSE curves obtained by the two algorithms. Form Fig. 3 we find that the RMSE of our TKF-FM is always smaller than that of TKF, which indicates the superiority of the proposed filtering algorithm in handling censored and fading measurements. This is because that our TKF-FM is capable of tackling the censoring and channel fading phenomena at the same time, while the TKF can not deal with fading measurements.

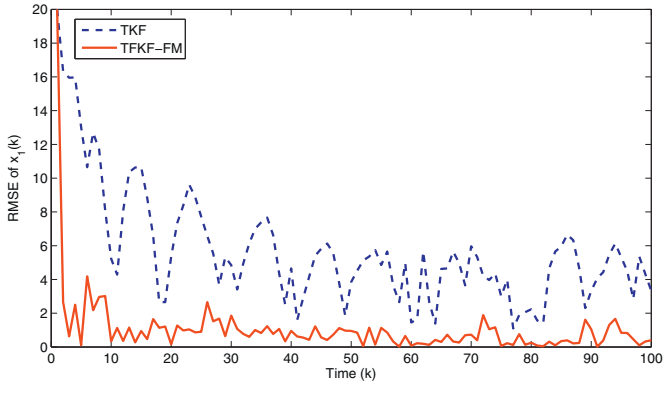

Fig. 3. Method comparison with [11] in RMSE1.

Theoretically, as time goes on, the RMSE of the TKF in Fig. 3 should degrade to a certain value beyond zero because that the TKF is unable to cope with the fading measurements. As to our TKF-FM, the RMSE should degrade to zero with the increase of k since the proposed TKF-FM can properly deal with the fading phenomenon. Nevertheless, this is often not true due to the fact that part of the measurement information is lost because of the fading phenomenon, which makes it difficult to recover the true state from the obtained fading measurements. This results in the situation that there is a small deviation between the obtained state estimate and the true state, and hence the RMSE of our TKF-FM in Fig. 3 can not degrade to zero as time goes on. goes on.

5. Conclusion

In this paper, we have investigated the recursive filtering problem for discrete time-varying systems in the coexistence of two important measurement nonlinearities, namely, censored and fading measurements. The fading measurements have been addressed under the assumption that the fading coefficients obey Gaussian distributions. The Gaussian distributions can be changed to other distributions, e.g., the uniform distribution on the interval $[\alpha_k, \beta_k]$ where $0 \le \alpha_k < \beta_k \le 1$. The adopted Lth-order Rice fading model not only covers the channel fading but also the time delay phenomena. The two phenomena have been carefully handled by introducing the expected values of the channel coefficients and the augmented states in the filter design, which have led to additional computations in the calculations of the filter gain matrix and the estimation error covariance. Fortunately, these additional computations are recursive or can be performed off-line. Accordingly, the designed filter is suitable for online applications. Finally, the effectiveness of the proposed filter has been illustrated by a numerical example.

In addition, related topics for further research work can be listed as follows.

- The Tobit Kalman estimation and filtering problem for linear systems with multiple network-induced phenomena, for example, packet dropouts, signal quantization, sensor saturations, and randomly occurring incomplete information.
- The Tobit Kalman estimation and filtering problem for nonlinear systems, especially when there are multiple types of nonlinearities in the system.
- The Tobit Kalman estimation and filtering problem for systems under different communication protocols, for instance, the round-robin protocol and the try-once-discard protocol.

Appendix A. Proof of Lemma 1

Proof. According to (4), the probability distribution of y_k^m with a normally distributed noise υ_k^m is as follows:

$$f(y_k^m|x_k) = \frac{1}{\sqrt{R_k^{m,m}}}\phi\left(\frac{y_k^m-\chi_k^m}{\sqrt{R_k^{m,m}}}\right)u(y_k^m-\mathcal{I}^m) + \delta(\mathcal{I}^m-y_k^m)\Phi\left(\frac{\mathcal{I}^m-\chi_k^m}{\sqrt{R_k^{m,m}}}\right), \tag{31}$$

where $\phi(\frac{y_k^m-\chi_k^m}{\sqrt{R_k^{m,m}}})$ and $\Phi(\frac{\mathcal{I}^m-\chi_k^m}{\sqrt{R_k^{m,m}}})$ are given by (15)–(16), $u(y_k^m-\mathcal{I}^m)$ is the unit step function, and $\delta(\mathcal{I}^m-y_k^m)$ is the Dirac delta function. Based on (31), we have the mathematical expectation and variance of y_k^m as follows:

$$\begin{aligned}&\mathbb{E}\left\{y_k^m|x_k,R_k^{m,m}\right\}\\ &= \mathrm{Prob}\left\{y_k^m>\mathcal{I}^m|x_k,R_k^{m,m}\right\}\mathbb{E}\left\{y_k^m|y_k^m>\mathcal{I}^m,x_k,R_k^{m,m}\right\}\\ &\quad+\mathrm{Prob}\left\{y_k^m=\mathcal{I}^m|x_k,R_k^{m,m}\right\}\mathbb{E}\{y_k^m|y_k^m=\mathcal{I}^m,x_k,R_k^{m,m}\}.\end{aligned} \tag{32}$$

From (32), we know that, to compute $\mathbb{E}\{y_k^m|x_k,R_k^{m,m}\}$, we need to calculate the probabilities and expected values in (32).

$$\begin{aligned}\mathrm{Prob}\left\{y_k^m>\mathcal{I}^m|x_k,R_k^{m,m}\right\} &= \mathrm{Prob}\left\{y_k^m>\mathcal{I}^m|x_k,R_k^{m,m}\right\}\\ &= \mathrm{Prob}\{(y_k^*)^m>\mathcal{I}^m|x_k,R_k^{m,m}\}\\ &= \mathrm{Prob}\{\chi_k^m+\upsilon_k^m>\mathcal{I}^m|x_k,R_k^{m,m}\}\\ &= \mathrm{Prob}\{\upsilon_k^m>\mathcal{I}^m-\chi_k^m|x_k,R_k^{m,m}\}\\ &= \Phi\left(\frac{\chi_k^m-\mathcal{I}^m}{\sqrt{R_k^{m,m}}}\right).\end{aligned} \tag{33}$$

Hence, we can easily obtain that

$$\begin{aligned}\mathbb{E}\left\{y_k^m|y_k^m>\mathcal{I}^m,x_k,R_k^{m,m}\right\} &= \frac{1}{\sqrt{R_k^{m,m}}}\int_{\mathcal{I}^m}^{+\infty} z_k^m\frac{\Phi\left(\frac{z_k^m-\chi_k^m}{\sqrt{R_k^{m,m}}}\right)}{1-\Phi\left(\frac{\mathcal{I}^m-\chi_k^m}{\sqrt{R_k^{m,m}}}\right)}d_{z_k^m}\\ &= \chi_k^m+\sqrt{R_k^{m,m}}\lambda\left(\frac{\mathcal{I}^m-\chi_k^m}{\sqrt{R_k^{m,m}}}\right),\end{aligned} \tag{34}$$

where $\lambda(\frac{\mathcal{I}^m-\chi_k^m}{\sqrt{R_k^{m,m}}})$ is given by (14). Similar to (33)–(34) , we can obtain

$$\mathrm{Prob}\{y_k^m=\mathcal{I}^m|x_k,R_k^{m,m}\} = \Phi\left(\frac{\mathcal{I}^m-\chi_k^m}{\sqrt{R_k^{m,m}}}\right), \tag{35}$$

$$\mathbb{E}\{y_k^m|y_k^m=\mathcal{I}^m,x_k,R_k^{m,m}\} = \mathcal{I}^m. \tag{36}$$

Putting (33)–(36) into (32) results in (11). It follows easily from (31) that $\mathrm{Var}\{y_k^m|x_k,y_k^m<\mathcal{I}^m,R_k^{m,m}\}=0$, and hence we have

$$\begin{aligned}\mathrm{Var}\left\{y_k^m|x_k,R_k^{m,m}\right\} &= \mathrm{Var}\left\{y_k^m|x_k,y_k^m>\mathcal{I}^m,R_k^{m,m}\right\}\\ &= \mathbb{E}\left\{(y_k^m)^2|y_k^m>\mathcal{I}^m,x_k,R_k^{m,m}\right\}\\ &\quad-\left(\mathbb{E}\left\{y_k^m|y_k^m>\mathcal{I}^m,x_k,R_k^{m,m}\right\}\right)^2\\ &= R_k^{m,m}\left[1-\varphi\left(\frac{\mathcal{I}^m-\chi_k^m}{\sqrt{R_k^{m,m}}}\right)\right],\end{aligned}$$

which is exactly the same as (12), where $\varphi(\frac{\mathcal{I}^m-\chi_k^m}{\sqrt{R_k^{m,m}}})$ is given by (13). The proof is now complete. □

Appendix B. Proof of Theorem 1

Proof. From the definition of $\hat{\xi}_{k|k-1}$, $\hat{\xi}_{k|k}$, $\mathcal{P}_{k|k-1}$ and $\mathcal{P}_{k|k}$, we can directly have (17)– (20) by applying the orthogonality projection principle in [48,49] to system (7)–(10) with the corresponding gain matrix given by (23). According to (11), we have

$$\hat{y}^m_{k|k-1} = \bar{\gamma}^m_k\left[\hat{\chi}^m_{k|k-1} + \sqrt{R^{m,m}_k}\lambda\left(\frac{\mathcal{I}^m - \hat{\chi}^m_{k|k-1}}{\sqrt{R^{m,m}_k}}\right)\right] + (1-\bar{\gamma}^m_k)\mathcal{I}^m. \tag{37}$$

Noting that $y_k = \mathrm{diag}\{y^1_k, y^2_k, \ldots, y^{n_y}_k\}$, we certainly have (21) from (37), where $\lambda(\frac{\mathcal{I}-\hat{\chi}_{k|k-1}}{\sqrt{R_k}})$ is given by (22). Subtracting (21) from (10) leads to

$$\tilde{y}_{k|k-1} = \Upsilon_k\theta_k\mathcal{C}_k\tilde{\xi}_{k|k-1} + \Upsilon_k\left(\upsilon_k - \lambda\left(\frac{\mathcal{I}-\hat{\chi}_{k|k-1}}{\sqrt{R_k}}\right)\mathcal{R}_k\right). \tag{38}$$

Substituting (38) into the definitions of $\Sigma_{\tilde{\xi}_{k|k-1}\tilde{y}_{k|k-1}}$ and $\Sigma_{\tilde{y}_{k|k-1}\tilde{y}_{k|k-1}}$, we have

$$\begin{aligned}\Sigma_{\tilde{\xi}_{k|k-1}\tilde{y}_{k|k-1}} &= \mathbb{E}\left\{\tilde{\xi}_{k|k-1}\tilde{y}^T_{k|k-1}\right\}\\ &= \mathbb{E}\left\{\tilde{\xi}_{k|k-1}\left(\Upsilon_k\theta_k\mathcal{C}_k\tilde{\xi}_{k|k-1} + \Upsilon_k\left(\upsilon_k - \lambda\left(\frac{\mathcal{I}-\hat{\chi}_{k|k-1}}{\sqrt{R_k}}\right)\mathcal{R}_k\right)\right)^T\right\}\\ &= \mathcal{P}_{k|k-1}\left(\bar{\Upsilon}_k\bar{\theta}_k\mathcal{C}_k\right)^T,\end{aligned}$$

which is exactly the same as (24), and

$$\begin{aligned}\Sigma_{\tilde{y}_{k|k-1}\tilde{y}_{k|k-1}} &= \mathbb{E}\left\{\tilde{y}_{k|k-1}\tilde{y}^T_{k|k-1}\right\}\\ &= \bar{\Upsilon}_k\bar{\theta}_k\mathcal{C}_k\mathcal{P}_{k|k-1}\left(\bar{\Upsilon}_k\bar{\theta}_k\mathcal{C}_k\right)^T\\ &\quad + \mathbb{E}\left\{\Upsilon_k\left(\upsilon_k - \lambda\left(\frac{\mathcal{I}-\hat{\chi}_{k|k-1}}{\sqrt{R_k}}\right)\mathcal{R}_k\right)\right.\\ &\quad \left.\times\left(\upsilon_k - \lambda\left(\frac{\mathcal{I}-\hat{\chi}_{k|k-1}}{\sqrt{R_k}}\right)\mathcal{R}_k\right)^T\Upsilon^T_k\right\}.\end{aligned} \tag{39}$$

For simplicity of the deduction, we assume that $\mathrm{cov}\{y^m_k, y^t_k\} = 0$ for $m \neq t$, $m, t = 1, 2, \ldots, n_y$. The generalization of the result to the case where $\mathrm{cov}\{y^m_k, y^t_k\} \neq 0$ for $m \neq t$ is straightforward but will bring notational burdens. Recalling the definition of the variance of y_k and noting (12), we have

$$\begin{aligned}&\mathbb{E}\left\{\Upsilon_k\left(\upsilon_k - \lambda\left(\frac{\mathcal{I}-\hat{\chi}_{k|k-1}}{\sqrt{R_k}}\right)\mathcal{R}_k\right)\left(\upsilon_k - \lambda\left(\frac{\mathcal{I}-\hat{\chi}_{k|k-1}}{\sqrt{R_k}}\right)\mathcal{R}_k\right)^T\Upsilon^T_k\right\}\\ &= \mathrm{Var}\{y_k|x_k, R_k\}\\ &= \mathrm{diag}\{\mathrm{Var}\{y^1_k|x_k, R^{1,1}_k\}, \ldots, \mathrm{Var}\{y^{n_y}_k|x_k, R^{n_y,n_y}_k\}\}\\ &= R_k\left[I - \varphi\left(\frac{\mathcal{I}-\hat{\chi}_{k|k-1}}{\sqrt{R_k}}\right)\right],\end{aligned} \tag{40}$$

where the second equality holds from the fact that $\mathrm{cov}\{y^m_k, y^t_k\} = 0$ for $m \neq t$ and $\varphi(\frac{\mathcal{I}-\hat{\chi}_{k|k-1}}{\sqrt{R_k}})$ is given by (26). Substituting (40) into (39), we have (25). The proof is now complete. □

References

[1] R. Caballero-Aguila, A. Hermoso-Carazo, J. Linares-Perez, Fusion estimation using measured outputs with random parameter matrices subject to random delays and packet dropouts, Signal Process. 127 (2016) 12–23.

[2] M. Basin, S. Elvira-Ceja, E. Sanchez, Mean-square h_∞ filtering for stochastic systems: application to a 2DOF helicopter, Signal Process. 92 (3) (2012) 801–806.

[3] X. Li, S. Sun, h_∞ Filtering for multiple channel systems with varying delays, consecutive packet losses and randomly occurred nonlinearities, Signal Process. 104 (2012) 109–121.

[4] Y. Zhang, P. Shi, S.K. Nguang, H.R. Karimi, Observer-based finite-time fuzzy h_∞ control for discrete-time systems with stochastic jumps and time-delays, Signal Process. 97 (2014) 252–261.

[5] G. Zhou, L. Wu, J. Xie, W. Deng, T. Quan, Constant turn model for statically fused converted measurement kalman filters, Signal Process. 108 (2015) 400–411.

[6] Y. Song, G. Wei, G. Yang, Distributed h_∞ filtering for a class of sensor networks with uncertain rates of packet losses, Signal Process. 104 (2014) 143–151.

[7] H. Wang, P. Shi, J. Zhang, Event-triggered fuzzy filtering for a class of nonlinear networked control systems, Signal Process. 113 (2015) 159–168.

[8] S. Kluge, K. Reif, M. Brokate, Stochastic stability of the extended kalman filter with intermittent observations, IEEE Trans. Autom. Control 55 (2) (2010) 514–518.

[9] S. Julier, J. Uhlmann, Unscented filtering and nonlinear estimation, Proc. IEEE 92 (3) (2004) 401–422.

[10] L. Li, Y. Xia, UKF-Based nonlinear filtering over sensor networks with wireless fading channel, Inf. Sci. 316 (2015) 132–147.

[11] B. Allik, C. Miller, M.J. Piovoso, R. Zurakowski, The Tobit Kalman filter: an estimator for censored measurements, IEEE Trans. Control Syst. Technol. 24 (1) (2016) 365–371.

[12] J. Buckley, I. James, Linear regression with censored data, Biometrika 66 (3) (1979) 429–436.

[13] T. Amemiya, Regression analysis when the dependent variable is truncated normal, Econometrica 41 (6) (1973) 997–1016.

[14] R. Carson, Y. Sun, The tobit model with a non-zero threshold, Econometrics J. 10 (3) (2007) 488–502.

[15] J. Tobin, Estimation of relationships for limited dependent variables, Econometrica 26 (1) (1958) 24–36.

[16] A. Assa, F. Janabi-Sharifi, A robust vision-based sensor fusion approach for real-time pose estimation, IEEE Trans. Cybern. 44 (2) (2014) 217–227.

[17] C. Rago, P. Willett, Y. Bar-Shalom, Censoring sensors: a low-communication-rate scheme for distributed detection, IEEE Trans. Aerosp. Electron.Syst. 32 (1) (1996) 554–568.

[18] S. Appadwedula, V.V. Veeravalli, D.L. Jones, Decentralized detection with censoring sensors, IEEE Trans. Signal Process. 56 (4) (2008) 1362–1373.

[19] C. Miller, B. Allik, M. Piovoso, R. Zurakowski, Estimation of mobile vehicle range & position using the tobit kalman filter, in: Proceedings of the IEEE Conference on Decision and Control, Los Angeles, California, USA, December, 2014, pp. 5001–5007.

[20] W. Li, Y. Jia, Tobit kalman filter with time-correlated multiplicative measurement noise, IET Control Theory Appl. 11 (1) (2017) 122–128.

[21] B. Ibarz-Gabardós, P.J. Zufiria, A kalman filter with censored data, in: IEEE International Workshop on Intelligent Signal Processing, Faro, Portugal, September, 2005, pp. 74–79.

[22] B. Allik, C. Miller, M.J. Piovoso, R. Zurakowski, Nonlinear estimators for censored data: a comparison of the EKF, the UKF and the tobit kalman filter, in: Proceedings of the American Control Conference , Chicago, IL, USA, July, 2015, pp. 5146–5151.

[23] J. Hampshire, J. Strohbehn, Tobit maximum-likelihood estimation for stochastic time series affected by receiver saturation, IEEE Trans. Inf. Theory 38 (2) (1992) 457–469.

[24] B. Allik, C. Miller, M.J. Piovoso, R. Zurakowski, Estimation of saturated data using the tobit kalman filter, in: Proceedings of the American Control Conference, Portland, Oregon, USA, June, 2014, pp. 4151–4156.

[25] Y. Mostofi, R.M. Murray, To drop or not to drop: design principles for kalman filtering over wireless fading channels, IEEE Trans. Autom. Control 54 (2) (2010) 376–381.

[26] H. Geng, Y. Liang, F. Yang, L. Xu, Q. Pan, Joint estimation of target state and ionospheric height bias in over-the-horizon radar target tracking, IET Radar, Sonar Navig. 10 (7) (2016) 1153–1167.

[27] H. Geng, Y. Liang, X. Zhang, The linear minimum mean square error observer for multi-rate sensor fusion with missing measurements, IET Control Theory Appl. 8 (14) (2014) 175–183.

[28] E. Biglieri, J. Proakis, S. Shamai, Fading channels: information-theoretic and communications aspects, IEEE Trans. Inf. Theory 44 (2619–2686) (1998).

[29] R. Berry, R. Gallager, Communication over fading channels with delay constraints, IEEE Trans. Inf. Theory 48 (5) (2002) 1135–1149.

[30] D. Ding, Z. Wang, J. Lam, B. Shen, Finite-horizon h_∞ control for discrete time–varying systems with randomly occurring nonlinearities and fading measurements, IEEE Trans. Autom. Control 60 (9) (2015a) 2488–2493.

[31] D. Ding, Z. Wang, B. Shen, H. Dong, Envelope-constrained h_∞ filtering with fading measurements and randomly occurring nonlinearities: the finite horizon case, Automatica 55 (2015b) 37–45.

[32] H. Dong, Z. Wang, S.X. Ding, H. Gao, On h_∞ estimation of randomly occurring faults for a class of nonlinear time-varying systems with fading channels, IEEE Trans. Autom. Control 61 (2) (2016) 479–484.

[33] S. Zhang, Z. Wang, D. Ding, H. Shu, Fuzzy filtering with randomly occurring parameter uncertainties, interval delays, and channel fadings, IEEE Trans. Cybern. 44 (3) (2014) 406–417.

[34] E. Garone, B. Sinopoli, A. Goldsmith, A. Casavola, LQG control for MIMO systems over multiple erasure channels with perfect acknowledgment, IEEE Trans. Autom. Control 57 (2) (2012) 450–456.
[35] S. Zhang, Z. Wang, D. Ding, H. Shu, Fuzzy control with randomly occurring infinite distributed delays and channel fadings, IEEE Trans. Fuzzy Syst. 22 (1) (2014) 189–200.
[36] N. Elia, Remote stabilization over fading channels, Syst. Control Lett. 54 (2005) 237–249.
[37] N. Xiao, L. Xie, L. Qiu, L, feedback stabilization of discrete-time networked systems over fading channels, IEEE Trans. Autom. Control 57 (9) (2012) 2176–2189.
[38] F. Ren, Y. Zheng, A novel emulator for discrete-time MIMO triply selective fading channels, IEEE Trans. Circuits Syst. I 57 (9) (2010) 2542–2551.
[39] A. Alimohammad, B.F. Cockburn, Modeling and hardware implementation aspects of fading channel simulators, IEEE Trans. Veh. Technol. 57 (4) (2008) 2055–2069.
[40] J. Hu, Z. Wang, H. Gao, Recursive filtering with random parameter matrices, multiple fading measurements and correlated noises, Automatica 49 (2013) 3440–3448.
[41] J. Zhang, L. Ma, Y. Liu, Passivity analysis for discrete-time neural networks with mixed time-delays and randomly occurring quantization effects, Neurocomputing 216 (2016) 657–665.
[42] Q. Li, B. Shen, Y. Liu, F.E. Alsaadi, Event-triggered h_∞ state estimation for discrete-time stochastic genetic regulatory networks with markovian jumping parameters and time-varying delays, Neurocomputing 174 (2016) 912–920.
[43] Y.S. Moon, P. Park, W.H. Kwon, Y.S. Lee, Delay-dependent robust stabilization of uncertain state-delayed systems, Int. J. Control 74 (14) (2001) 1447–1455.
[44] E. Fridman, U. Shaked, A descriptor system approach h_∞ control of linear time-delay systems, IEEE Trans. Autom. Control 47 (2) (2002) 253–270.
[45] M. Wu, Y. He, J. She, G. Liu, Delay-dependent criteria for robustst ability of time-varying delay systems, Automatica 40 (8) (2004) 1435–1439.
[46] J. Hu, Z. Wang, H. Gao, L.K. Stergioulas, Robust sliding mode control for discrete stochastic systems with mixed time-delays, randomly occurring uncertainties and randomly occurring nonlinearities, IEEE Trans. Ind. Electron. 59 (7) (2012) 3008–3015.
[47] B. Allik, M. ILG, R. Zurakowski, Ballistic roll estimation using EKF frequency tracking and adaptive noise cancellation, IEEE Trans. Aerosp. Electron.Syst. 49 (4) (2013) 2546–2553.
[48] B.D.O. Anderson, J.B. Moore, Optimal Filtering, Prentie-hall, Inc., Englewood Cliffs, N. J., 1979.
[49] S. Haykin, Adaptive Filter Theory, Prentice-Hall, New Jersey, NJ, USA, 2002.